Ocean Systems Engineering, *Vol. 14, No. 3 (2024) 261-276*
https://doi.org/10.12989/ose.2024.14.3.261

Parametric investigation involving response reduction for a semi-submersible floater with shape alteration, stepping, and tilting of columns and pontoons

Anand B. Vishnu[a] and Abdul M. Akbar[*]

Department of Civil Engineering, NIT Calicut, Kerala, India

(Received April 20, 2024, Revised August 20, 2024, Accepted September 10, 2024)

Abstract. Numerical investigation was carried out to analyze the hydrodynamic response of 4-column semi-submersible floaters, incorporating variations such as stepping and alterations in the shape/geometry of columns and pontoons, as well as tilting of main columns. Utilizing Ansys-AQWA, a hydrodynamic software based on panel method, simulations were executed for these scenarios. The simulations yielded insights into responses, excitation forces/moments, and pressure on the structure, facilitating a comparison between the models through a parametric study. It was observed that stepping of pontoons and tilting of columns led to reduced responses, forces, and pressures, reaching balance through appropriate stepping and tilting. Additionally, altering the geometry of columns and pontoons indicated the potential benefits of employing elliptical pontoons and pentagonal columns for enhanced response control.

Keywords: hydrodynamic; panel method; parametric; response control; semi-submersible; stepping; tilting

1. Introduction

The offshore wind power generation sector is becoming increasingly relevant due to the escalating demand for cleaner energy. Unlike many other sectors profoundly affected by the COVID pandemic, the offshore wind industry remained resilient throughout 2020, with Europe maintaining its lead in total capacity. The Global Offshore Wind Report 2023 forecasts that 380 GW of offshore wind power generating facility to be complete by 2030. By meeting the growing demand for clean energy, we can significantly advance our energy transition and environmental objectives. Floating platforms are indispensable, especially in deeper seas and farther from the coast, where wind resource potential is typically greater. Among various floating platforms, the semi-submersible platform stands out in three key areas: first, it can be assembled onshore and then towed to its final location, ready for immediate use; second, its mooring systems are cost-effective; and third, it experiences minimal downtime in operational sea states due to reduced platform motion. Most of the existing research on floating offshore wind turbines are using the Horizontal Axis Wind Turbine (HAWT), proposed by Jonkman *et al.* (2009) with spar, TLP and semi-submersible as platforms.

*Corresponding author, Assistant Professor, E-mail: maa@nitc.ac.in
[a]M.Tech Student, E-mail: anandvishnub@yahoo.com

http://www.techno-press.org/?journal=ose&subpage=7 ISSN: 2093-6702 (Print), 2093-677X (Online)

Due to its significant loads, the conventional HAWT encounters numerous challenges when deployed offshore. An alternative to the traditional HAWT is the Vertical Axis Wind Turbine (VAWT), such as the Darrieus H-rotor, which boasts a higher safety margin for mooring systems in intense wave conditions. Unlike the conventional semi-submersibles used for rigs, the pontoon structure of a wind turbine-holding semi-submersible operates independently from the main columns. The columns are supported by a simple prismatic shape, while bracings will connect the pontoons and columns. The major emphasis will be on heave and pitch stabilisation as the objective of response control depends heavily on this two degrees of freedom. Heave plates, VIV suppressors, etc can be used to achieve these but all of which will only increase the added mass. So the idea of shape upgradation comes into picture. Shape and mooring line orientation studies have already been done by Sharma *et al.* (2014) on conventional semi-submersible. Various shapes, including square, elliptical, circular, hexagonal, pentagonal, and octagonal, can be utilized for both columns and pontoons. The effect of stepping on a spar platform supporting a wind turbine has been done by Sethuraman and Venugopal (2013). Stepping along the longitudinal axis of the pontoons and columns can also be implemented to alleviate pressure on the structure.

Another approach to reduce structural strain is to angle the primary columns outward as done by Liu *et al.* (2019) on 3-C semi-submersible. The effects of these modifications, including stepping, tilting, and changes in shape, can be comprehensively assessed through experimental studies conducted in a wave flume or basin. However, such investigations require significant financial resources, time, and specialized equipment. Consequently, the emphasis is placed on numerical simulations using software. Simulation-based designs allow for the alteration of parameters to analyse their impact on responsiveness, excitation characteristics, pressure distribution, and other performance and stability attributes. According to Ma *et al*. (2019), for a semi-submersible supporting a wind turbine heave, pitch and roll are the most significant responses that should be considered during analysis and upgradation. The reduction of the semi-submersible's motion necessitates thorough research into both pontoon and column configurations.

As the earlier studies highlight the advantages of stepping of spar platform on the response reduction, tilting of main columns of 3 column semi-submersibles, the benefits of four column semi-submersible over a 3 column semi-submersible; a further analysis into stepping of column and pontoon members of a semi-submersible platform and tilting of main columns of 4 column semi-submersibles can be done. Also the column and pontoon geometry is subjected to different shape alterations to shows its effect on subsequent response reduction. The idea of finding the effect of stepping and tilting on a semi-submersible is done on a preliminary design stage to save computational time and money while doing detailed CFD study. Also the CFD study involving the aerodynamic part as well as the optimization involving use of the cost function is considered as an extension of the work.

2. Model and numerical simulation

2.1 Model description

One of the primary works involving a parametric study of semi-submersible supporting wind turbine was carried out by Shokouhian *et al*. (2021). A novel platform using inclined leg over a conventional semi-submersible to reduce heave resonance was done using Zhang *et al*. (2022). The semi-submersible platform considered for this study comprises four primary columns and a central

Table 1 Geometric, mass and hydrostatic details of the semi-submersible with VAWT

Description	4-C semi-submersible with VAWT
Blade length (m)	63.5
Weight of VAWT (kg)	1539000
Tower height (m)	33.6
Draft (m)	24.75
Main Column diameter (m)	11.25
Column height (m)	30
Hexagonal pontoon edge length (m)	12.37
Hexagonal pontoon height (m)	7.5
Brace diameter (m)	2.25
Displacement (kg)	2.10×10^7
Moment of inertia I_{xx}, I_{yy} ($kg.m^2$)	2.46×10^{10}
Moment of inertia I_{xy} ($kg.m^{2)}$	2.95×10^{10}
Number of mooring lines	4
Un-stretched line length (m)	886
Water depth (m)	187.5
Depth, Radius of fairlead (m)	20.98, 49.98

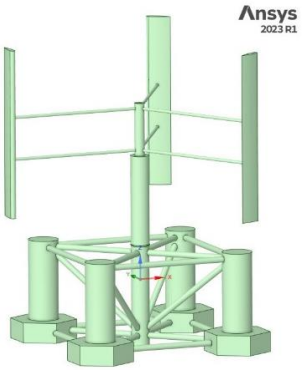

Fig. 1 (a) 3D model of the semi-submersible floater in Ansys Spaceclaim

column with a circular cross-section as done in the study done by Rajeswari and Nallayarasu (2021). Hexagonal pontoons are affixed at the base of the main columns, with bracings linking the columns and pontoons together. The Vertical Axis Wind Turbine (VAWT) being studied is of the Darrieus type H-rotor, positioned atop the central column. The suitability of such a 4-C semi-submersible floater along the Indian west coast has been studied by Rajeswari and Nallayarasu (2022). Fig. 1(a) shows the 3D model of the floater with wind turbine drawn using Ansys Spaceclaim. The geometric and hydrostatic specifications of both the semi-submersible and the VAWT are provided in Table 1. After modelling, it is further thinned as panels of negligible thickness and sliced at the waterline using Ansys Design Modeler. The modelling part ends with successfully loading the model into Ansys Workbench within the geometry component of the Hydrodynamic Diffraction module.

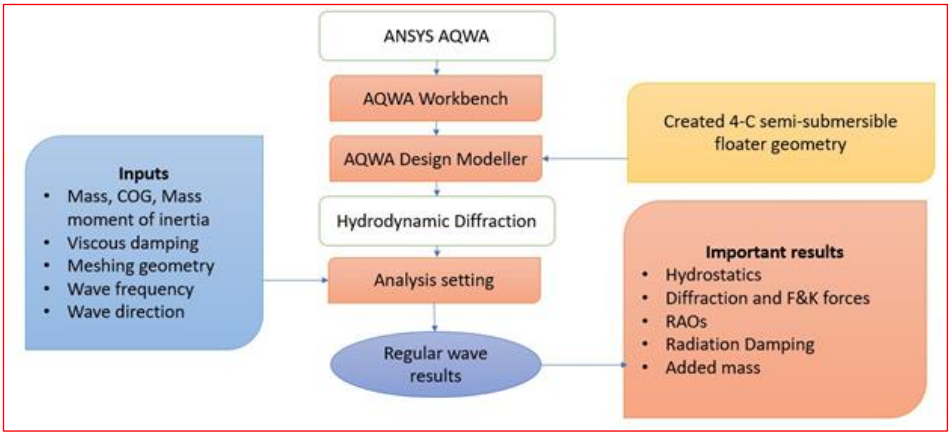

Fig. 1 (b) Flowchart showing numerical simulation in ANSYS AQWA

2.2 Numerical simulation

Otter *et al.* (2022) comparatively studied different approaches for numerical analysis of floating offshore wind turbines. From this paper, the different ideologies behind every software including its merits, demerits and scope of each with regard to its fidelity range can be comparatively studied. As suggested by A. Subbulakshmi *et al.* (2022), for pre-design and sizing requirements the use of uncoupled and low fidelity coupled analysis can be used instead of High fidelity fully coupled CFD-FEM fluid structure interaction analysis. Numerical simulations were carried out to analyze the hydrodynamic response of 4-column (4-C) semi-submersibles supporting a Vertical Axis Wind Turbine (VAWT) using Ansys-AQWA. This software employs radiation and diffraction techniques in three dimensions to solve boundary integral equations. The geometry of the 4-C semi-submersible was modeled using Ansys Design Modeler. The numerical method utilized the Panel method for all components of the floater, including the braces, treating all elements as diffracting entities. Finite depth effects were accounted for in the simulations by replicating the dimensions of the wave tank, including water depth.

The governing equation for potential flow is the Laplace equation.

$$\nabla^2 \phi = 0 \tag{1}$$

The governing equation of a floating body in six degrees of motion is given as

$$[M+A]\{\ddot{X}\} + [B]\{\dot{X}\} + [C]\{X\} = \{F\} \tag{2}$$

where, ϕ is the velocity potential, M is mass matrix, A is the added mass, B is the damping matrix, C is the restoring coefficient, F is the hydrodynamic force vector due to incident wave, X, $\dot{X}$ and $\ddot{X}$ are displacement, velocity and acceleration vectors respectively.

After modelling and loading it into the Hydrodynamic analysis module of Ansys AQWA, we can give the domain and boundary conditions, mooring conditions, point loads, geometric parameters and damping values. Since AQWA cannot solve viscous damping, a significant amount of damping is given as an additional part so as to counter this effect. In the study 95% of the total damping is

Table 2 Dimensions details of different sections of the stepped column (SC- stepped column)

Stepped Column	Dimension of stepped section
2SC	D_1= 11 m ; D_2 = 11.5 m ; V_2= 2983.53 m^3
3SC	D_1= 11 m ; D_2 = 11.25 m ; D_3 = 11.5 m ; V_3= 2983.04 m^3
4SC	D_1= 11 m ; D_2 = 11.17 m ; D_3 = 11.33 m ; D_4 = 11.5 m ; V_4= 2982.87 m^3
5SC	D_1= 11 m ; D_2 = 11.125 m ; D_3 = 11.25 m ; D_4 = 11.375 m ; D_5 = 11.5 m ; V_5= 2982.79 m^3

where, D_n is the diameter of the column section considered for each height and V_n is total volume

due to viscous part and only the remaining is considered as radiation damping as done in the works of Rajeswari and Nallayarasu (2021). Such a linearization of the viscous damping part is essential to adopt this method as an advancer step to reduce simulation time and come up with only essential models that need CFD analysis. This assumptions therefore adopts a linear additional viscous damping component given as corrector step after finding the radiation damping. The flowchart showing procedure for numerical simulation in ANSYS AQWA is shown in Fig. 1(b).

3. Result and discussion

By varying the different component geometries and by introducing stepping and tilting, a good number of models are tested numerically and the results of these analysis are provided in this section.

3.1 Stepping of columns and pontoons

The columns are modelled in such a way that the longitudinal cross section is varied in the form of steps. The number of steps in the column being varied from two to five, the volume of the column is being kept a constant throughout for uniform comparison. Fig. 2(a) shows the different stepped column and pontoon geometries considered in the study. The volume and section diameter details of two to five stepped column semi-submersibles is given in Table 2.

The total column length is considered to be a constant throughout the different stepping cases.

Original volume (without stepping), V_1= 2983 m^3.

The pontoons are modelled such that the longitudinal cross-section is varied in the form of steps. The number of steps in the pontoon being varied from two to five, the volume of the pontoon is being kept a constant throughout. The volume and side length details of two to five stepped pontoon semi-submersibles is given in Table 3. Table 4 gives a comparison of RAO, excitation force, moment and pressure acting with column and pontoon stepping.

Original volume (without stepping) V_1= 2981.62 m^3.

The Response Amplitude Operator (RAO) which is the ratio of Response in a direction to the Wave Amplitude, is found in three degrees of freedom; surge, heave and pitch. Also the excitation force and moment in heave and pitch directions are also found. The resonant peak amplitude values of the responses and excitation components are given in Table 3.

One representative panel discretization in case of 3 stepped column and 3 stepped pontoon is shown in Fig. 2(b) and 2(c) as follows. It shows the mesh size of 0.78m chosen after conducting convergence studies.

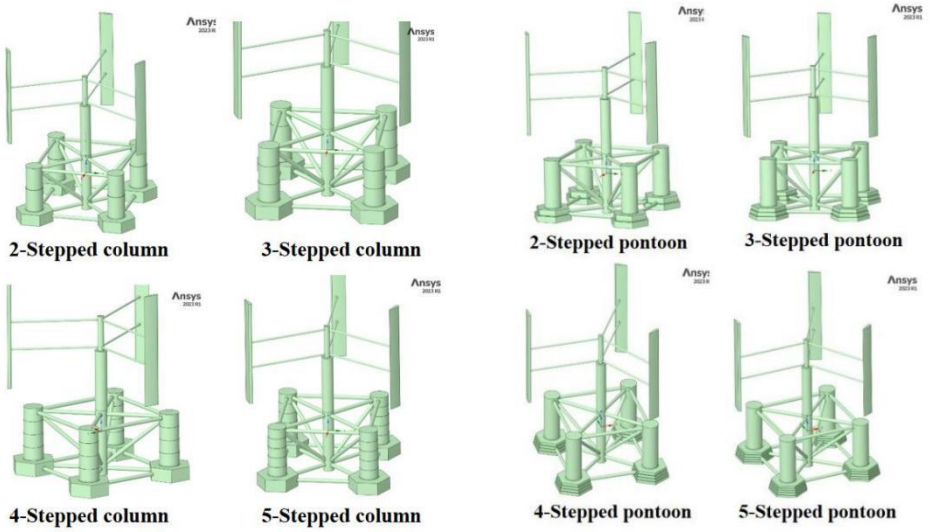

Fig. 2 (a) Different stepped column and pontoon geometries considered in the study

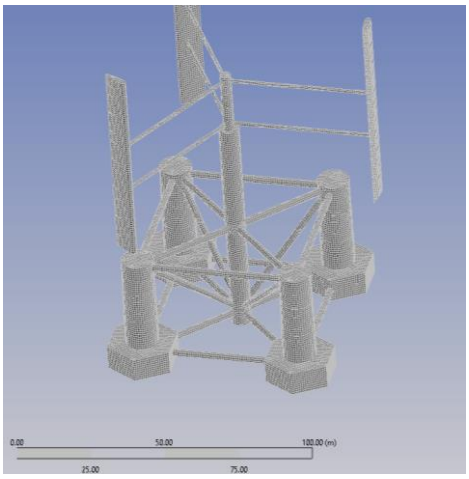

Fig. 2 (b) 3 stepped column panel discretization

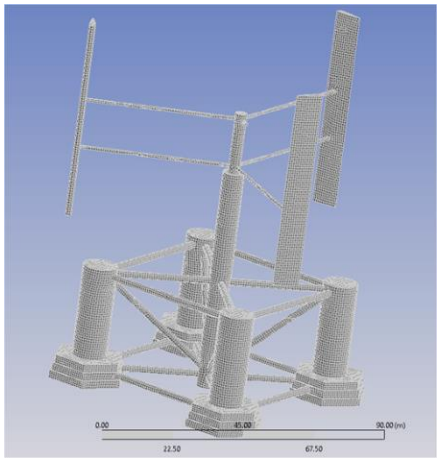

Fig. 2 (c) 3 stepped pontoon panel discretization

Table 3 Dimensions details of different sections of the stepped pontoon (SC- stepped pontoon)

Stepped Pontoon	Dimension of stepped section
2SP	S_1= 11.54 m ; S_2 = 13.19 m ; V_2= 2994.63 m^3
3SP	S_1= 11.54 m ; S_2 = 12.36 m ; S_3 = 13.19 m ; V_3= 2990.23 m^3
4SP	S_1= 11.54 m ; S_2 = 12.09 m ; S_3 = 12.65 m ; S_4 = 13.20 m ; V_4= 2991.44 m^3
5SP	S1= 11.54 m ; S_2 = 11.96 m ; S_3 = 12.37 m ; S_4 = 12.78 m ; S_5 = 13.20 m ; V_5= 2990.71 m^3

Where S_n is the side length of the hexagonal pontoon at different heights and V_n is total volume

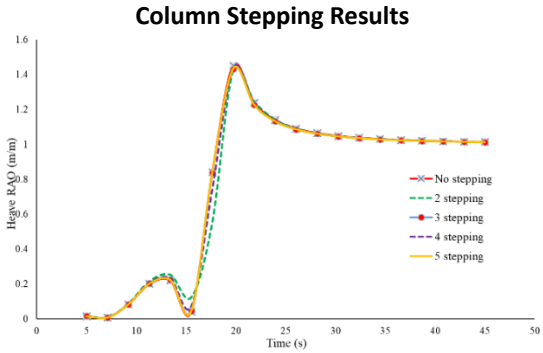

Fig. 3 (a) Heave RAO (m/m)

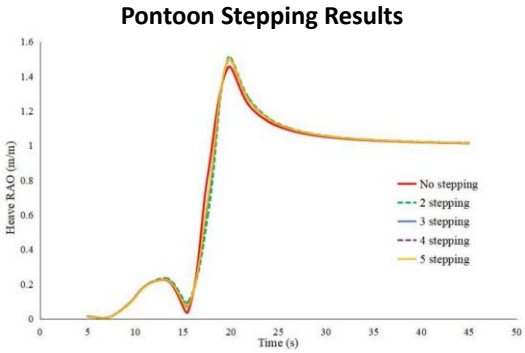

Fig. 3(b) Heave RAO (m/m)

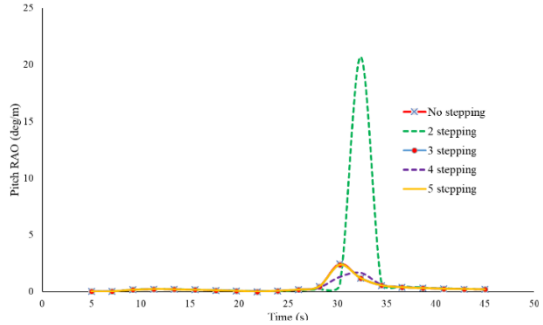

Fig. 3(c) Pitch RAO (deg/m)

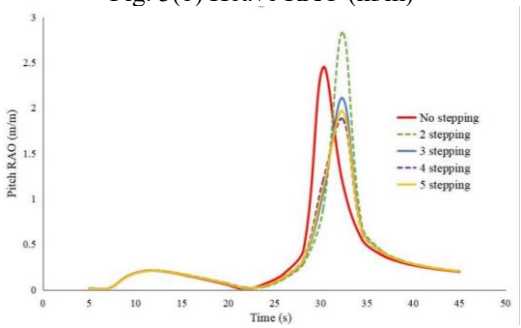

Fig. 3(d) Pitch RAO (deg/m)

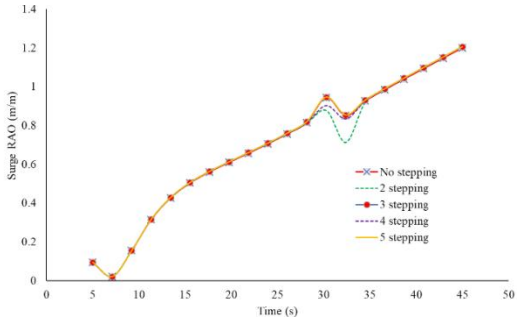

Fig. 3(e) Surge RAO (m/m)

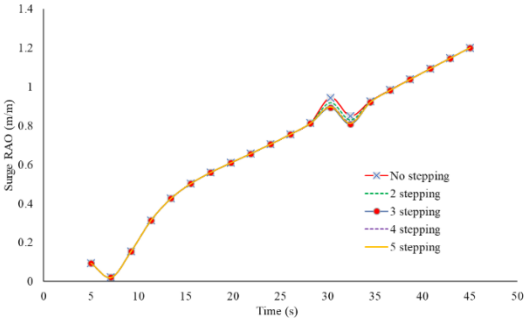

Fig. 3(f) Surge RAO (m/m)

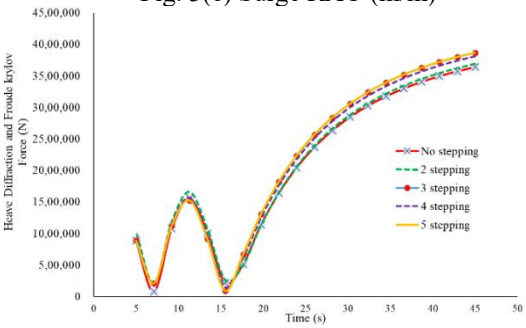

Fig. 3(g) Heave excitation (N)

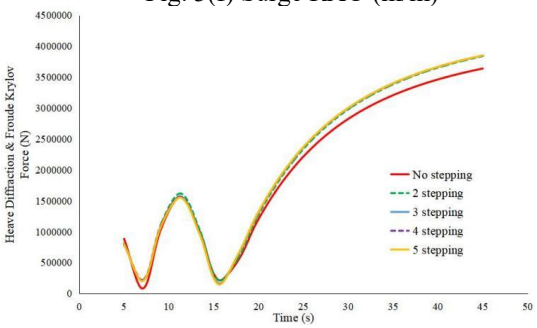

Fig. 3(h) Heave excitation (N)

Continued-

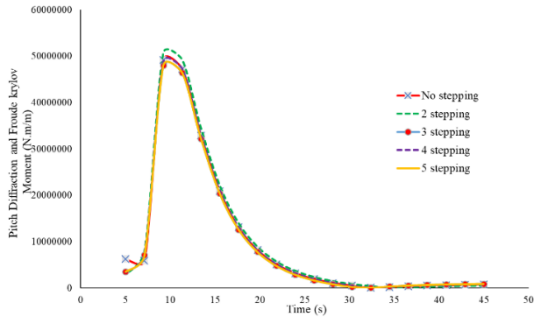

Fig. 3(i) Pitch moment (N.m/m)

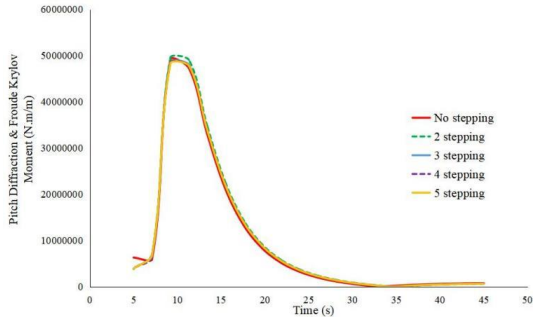

Fig. 3(j) Pitch moment (N.m/m)

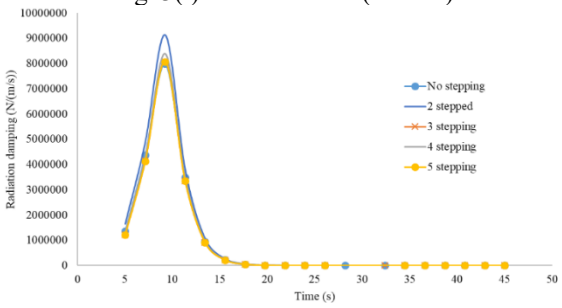

Fig. 3(k) Radiation damping (N/(m/s))

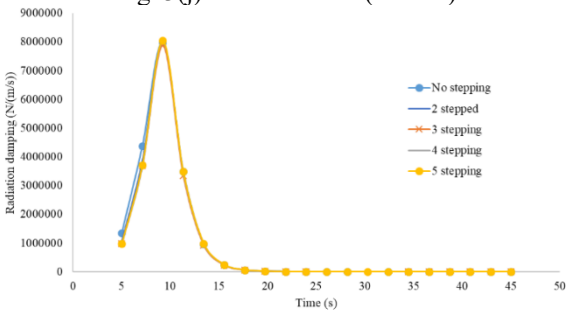

Fig. 3(l) Radiation damping (N/(m/s))

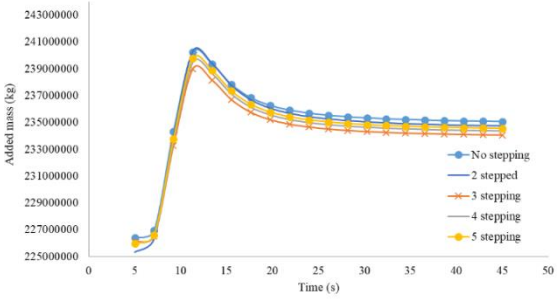

Fig. 3(m) Added mass (kg)

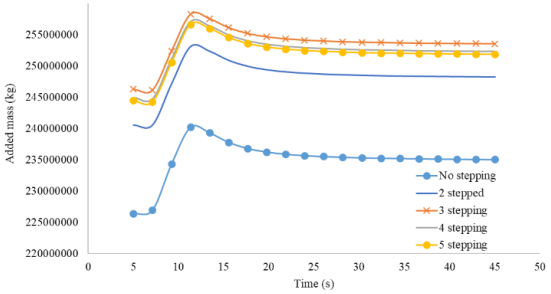

Fig. 3(m) Added mass (kg)

Table 4 Comparison of RAO, excitation force, moment and pressure acting with column and pontoon stepping. (SC- stepped column, SP- stepped pontoon)

Stepping	Heave RAO (m/m)	Pitch RAO (m/m)	Surge RAO (m/m)	Heave Excitation force (N/m)	Pitch excitation moment (N.m/m)	Max. Pressure in terms of head of water (m)
2SC	1.425	20.691	1.207	3690035	50720948	0.18582
3SC	1.4382	2.365	1.206	3864410	48076760	0.16918
4SC	1.4372	2.361	1.205	3806461	48843052	0.17425
5SC	1.434	2.382	1.204	3865025	48033512	0.16913
2SP	1.5078	2.828	1.199	3838756	49597704	0.17926
3SP	1.4997	2.1074	1.198	3846449	48623820	0.17739
4SP	1.4946	1.8794	1.200	3847919	48587040	0.17693
5SP	1.4974	1.9639	1.199	3849129	48358412	0.17685

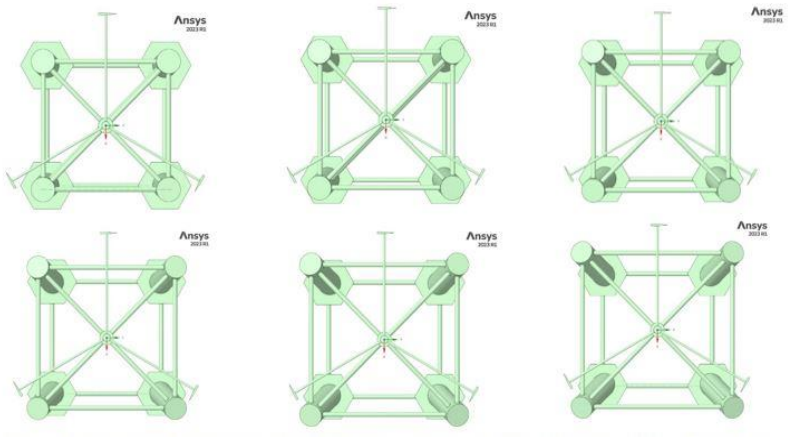

Fig. 4 Plan view of semi-submersible with inclination of columns from 0° to 30°

Figs. 3(a)-3(h) shows the Heave and Pitch RAO, Heave and Pitch excitation parameters for column and pontoon stepping.

From Table 4, it is clear that the heave response reduction for column stepping falls within the range of 2-3% for column stepping. Pitch response reduces with stepping of column, where 4 SP shows around 25% reduction. From Figs. 3(c) and 3(d) it is evident that 2SC has a resonant pitch amplitude of 20.7 around 33s which matches the natural period of the two stepped floater. The unusual peak observed needs further CFD test to understand the physics behind the abnormality.

The possible explanation to such a occurring will be owing to the fact that the 2SC must be focusing the wave energy, increasing the force and motion response in pitch degree. The shift in natural frequency and the excitation moment is due to the fact that the change in stiffness and mass distribution and associated change in mode shape which affects the boundary conditions and subsequently changing the natural frequency. Also as the change in geometry affects the added mass, it leads to change in the excitation moment as well.5SC & 4SP have the highest reduction in Heave excitation force which is around 8% and 4% respectively. 5SC & 5SP have the highest reduction in Pitch excitation moment which is around 42% for both. 5SC & 5SP have highest reduction in Maximum Pressure which is around 11% and 7% respectively. The stepped member concept for a semi-submersible aids in (a) reducing the chances of capsizing as it provides lower center of gravity (b) reducing the motion responses and enabling to operate in harsher weather conditions (c) reducing the risk of accidents and injuries and creating safer work environment (d) long term cost savings through reduced downtime, improved efficiency and extended equipment life.

3.2 Tilting of main columns

The primary columns of the semi-submersible floater are deliberately inclined from zero to a permissible degree of tilt. This tilted column configurations are analyzed in AQWA to determine the resulting response, excitation force, moment, and maximum pressure exerted. The inclination of the main columns is systematically varied from 0° to 30° in 5° increments, and the corresponding Heave and Pitch RAOs (Response Amplitude Operators) along with excitation force, moment, and maximum pressure are calculated, mirroring the process employed for stepping configurations. Fig.

Table 5 Comparison of peak RAOs, excitation force, moment and maximum pressure with change in angle of column tilt

Column tilt	Heave RAO (m/m)	Pitch RAO (m/m)	Surge RAO (m/m)	Heave Excitation force (N/m)	Pitch excitation moment (N.m/m)	Max. Pressure in terms of head of water (m)
0°	1.4518	2.4451	1.1999	4012312	50194224	0.1895
5°	1.4137	6.3284	1.2032	3907328	49006996	0.1522
10°	1.3722	6.3990	1.2072	3957252	51689524	0.1389
15°	1.3322	2.6763	1.2105	4031942	55698996	0.1300
20°	1.2754	1.7940	1.2194	4128729	61084356	0.1218
25°	1.2065	1.7128	1.2315	4318891	66971204	0.1121
30°	1.1400	2.6881	1.2449	4522175	75484408	0.1040

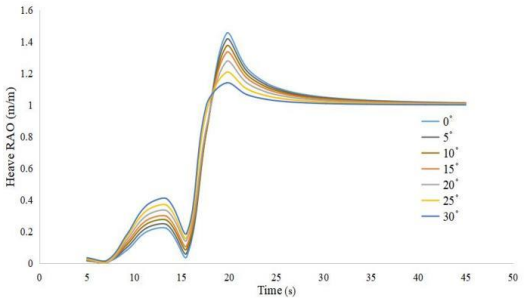

Fig. 5(a) Heave RAO (m/m)

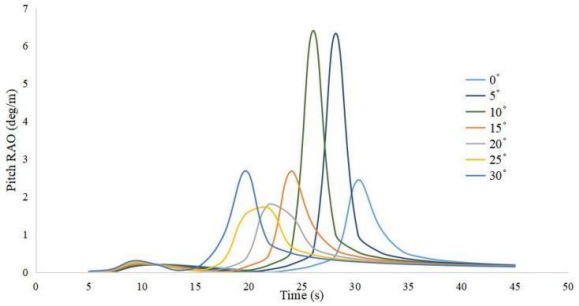

Fig. 5(b) Pitch RAO (deg/m)

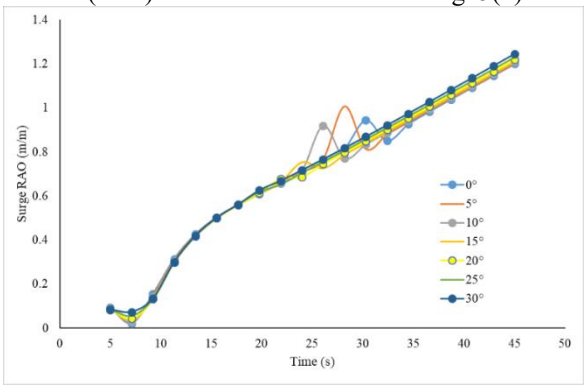

Fig. 5(c) Surge RAO (m/m)

4 shows the plan view of semi-submersible with inclination of columns from 0° to 30°. Table. 5 gives a comparison of peak RAOs, excitation force, moment and maximum pressure with change in column tilt. Figs. 5(a)-5(d) shows the Heave RAO, Pitch RAO, Heave excitation force, and Pitch moment in case of column tilting.

As the angle of column tilt increases there is negligible increase in the mass moment of inertia. The effect of this increase is countered in the solver itself. The decrease in the wave pressure as the column tilt happens, can be noted from Table 5.

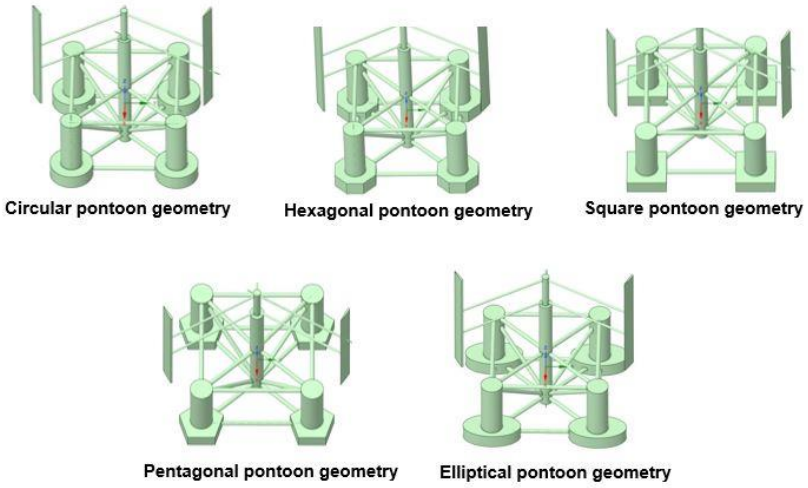

Fig. 6 Different pontoon geometries considered in the study

Table 6 Comparison of peak RAOs, excitation force, moment and maximum pressure with change in pontoon geometry

Shape of Pontoon	Heave RAO (m/m)	Pitch RAO (m/m)	Heave Excitation force (N/m)	Pitch excitation moment (N.m/m)	Max. Pressure in terms of head of water (m)
Hexagon	1.4841	2.2552	3638152	49194224	0.1495
Circular	1.4537	4.1226	3880774	47260576	0.1483
Square	1.4368	4.1640	3886671	47097972	0.1463
Ellipse	1.4350	2.1215	3890217	45773652	0.1439
Pentagon	1.7136	2.1512	3857119	47681900	0.1746
Octagon	1.4521	3.0041	3878137	47815616	0.1486

From Fig. 5(a) to Fig. 5(e), as the column is tilted through 30° there is a clear reduction in Heave Response by almost 22% and for 25°, a reduction in Pitch response by almost 30%. As the column is tilted from 0° to 5° there is a reduction in heave and pitch response and excitation parameters, but as the angle of tilt increases from 5° to 10° there is an increase in pitch response and excitation moment, which affects the heave excitation force as well showing similar trend for it as well. There is almost 45% reduction in maximum pressure head when tilted from 0° to 30°. Preferable angle of tilt stands at around 7.5° showing minimal response and excitation characteristics.

3.3 Pontoon shape alteration

The impact of altering pontoon geometry is meticulously examined following the prior study on pontoon stepping, with the volume held constant. Various pontoon shapes including circular, square, ellipse, pentagon, and octagon are meticulously compared to the existing hexagonal pontoon. Among these additional shapes, three (circle, square, and octagon) exhibit symmetrical characteristics along both axes, while the remaining two (ellipse and pentagon) demonstrate

asymmetry along the axes. Fig. 6 shows the different pontoon geometries considered in the study. The study also investigates the effects of this asymmetry difference. Given that the original model features a hexagonal pontoon shape, it is imperative to maintain its base area and volume while transitioning shapes. Height, volume, and area are kept constant, with only the surface shape of the pontoon being altered. Table 6 gives a comparison of peak RAOs, excitation force, moment and maximum pressure with change in pontoon geometry. The dimensions provided ensure consistency in both area and volume.

Hexagonal geometry
Base area = 397550000 mm^2
Volume = 29816225000 mm^3
Height = 7500 mm
Circular geometry
Diameter = 22498.36 mm
Pentagonal geometry
Side length = 15190 mm
Side length = 15190 mm
Square geometry
Side length = 19938.65 mm
Elliptical geometry
Semi major axis length = 15000 mm
Semi minor axis length = 8436.27 mm

Figs. 7(a)-7(d) shows the Heave RAO, Pitch RAO, Heave excitation force, and Pitch moment for change in pontoon geometry.

From Table 6 it is clear that the Elliptical shape has the lowest excitation moment when compared to other shapes with square shape coming second in that order. Elliptical shape shows 7% reduction in pitch moment and 10% reduction in pressure. Square shape shows 4% reduction in pitch moment and 3% reduction in pressure. Further those shapes having biaxial symmetry shows a peak values in pitch response and moment. Both elliptical and square shapes can be suggested to be used to control responses.

3.4 Column shape alteration

The impact of altering column geometry is thoroughly examined following the previous study on column stepping, with volume held constant. Various column shapes including circular, square, ellipse, pentagon, and octagon are meticulously compared to the existing circular column shape. Among these additional shapes, two (square and octagon) demonstrate symmetry along both axes, while the remaining three (hexagon, ellipse, and pentagon) exhibit different symmetry along both

Table 7 Comparison of peak RAOs, excitation force, moment and maximum pressure with change in column geometry

Shape of Column	Heave RAO(m/m)	Pitch RAO(m/m)	Heave Excitation force (N/m)	Pitch excitation moment (N.m/m)	Max. Pressure in terms of head of water (m)
Circular	1.4841	2.2552	3638151.5	49194224	0.1585
Hexagon	1.4448	3.0099	3890133.7	47553992	0.1485
Square	1.4448	2.7308	3881308.7	47735624	0.1486
Ellipse	1.4541	1.8018	3858117.7	47797948	0.1508
Pentagon	1.4438	3.0336	3890024	47530724	0.1482
Octagon	1.4696	1.6413	3799508	48136388	0.1532

axes. Fig. 8 shows the different column geometries considered in the study. The study also investigates the effects of this asymmetry difference. Given that the original model features a circular column shape, it is essential to maintain its base area and volume while transitioning shapes. Height, volume, and area are kept constant, with only the column base area shape being altered. Table 7 gives a comparison of peak RAOs, excitation force, moment and maximum pressure with change in column geometry. The provided dimensions ensure consistency in both area and volume.

MAIN COLUMNS
Circular geometry
Diameter=11250 mm
Base area = 99401955.05 mm^2
Height=30000 mm
Hexagonal geometry
Side length = 6185.45 mm
Elliptical geometry
Semi major axis length = 6328.12 mm
Semi minor axis length = 5000 mm
Pentagonal geometry
Side length = 7601.04 mm
Octagonal geometry
Side length = 4537.27 mm
Square geometry
Side length = 9970.05 mm

CENTRAL COLUMN
Circular geometry
Diameter = 6750 mm
Base area = 35784703.82 mm^2
Height = 37500 mm
Hexagonal geometry
Side length = 3711.27 mm
Elliptical geometry
Semi major axis length = 3796.87 mm
Semi minor axis length = 3000 mm
Pentagonal geometry
Side length = 4560.62 mm
Octagonal geometry
Side length = 2722.36 mm
Square geometry
Side length = 5982.03 mm

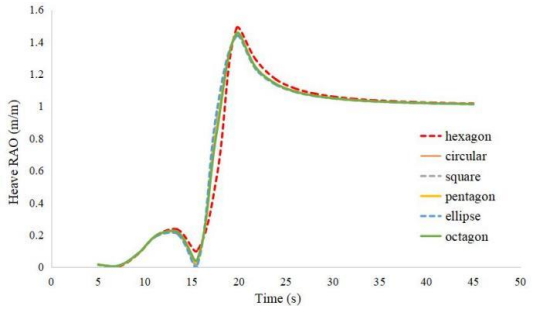

Fig. 7(a) Heave RAO (m/m)

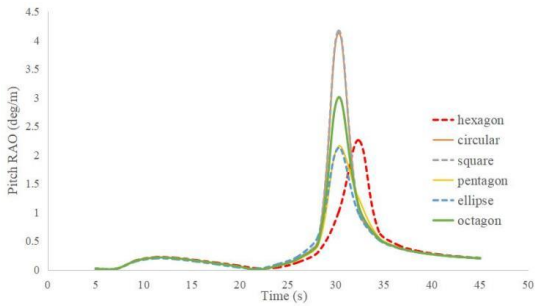

Fig. 7(b) Pitch RAO (deg/m)

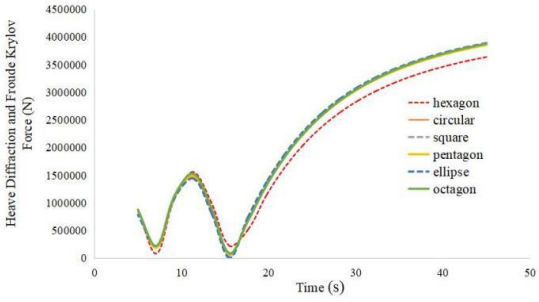

Fig. 7(c) Heave excitation force (N)

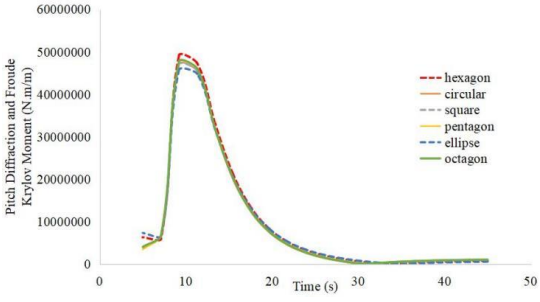

Fig. 7(d) Pitch moment (N.m/m)

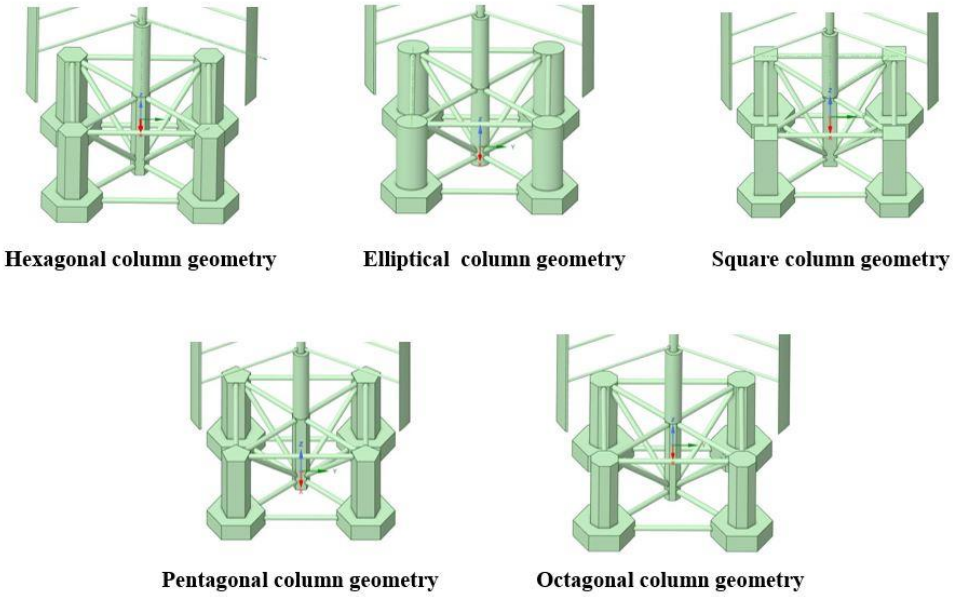

Fig. 8 Different column geometries considered in the study

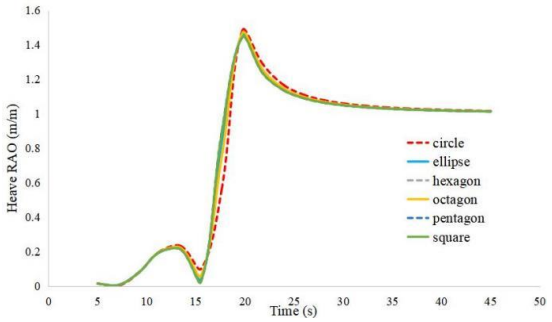

Fig. 9(a) Heave RAO (m/m)

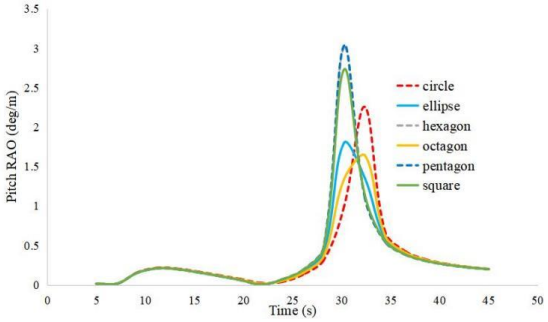

Fig. 9(b) Pitch RAO (deg/m)

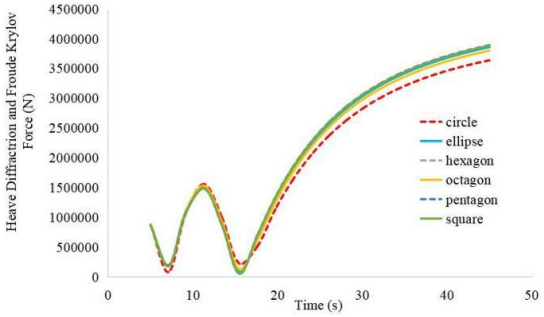

Fig. 9(c) Heave excitation force (N)

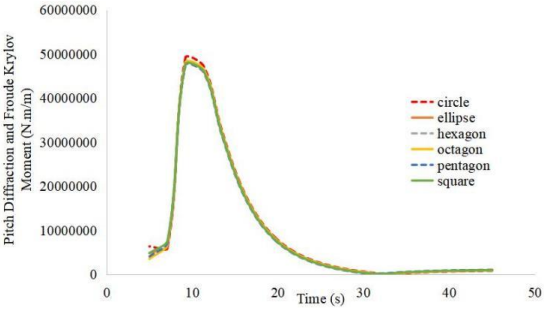

Fig. 9(d) Pitch moment (N.m/m)

Figs. 9 (a)-9(d) shows the Heave RAO, Pitch RAO, Heave excitation force and Pitch moment for different column geometries. Both the central column and the main column shapes are changed and then the effect of the shape alteration is studied.

From Table 7 it is clear that the Pentagonal column shows 3% reduction in heave response and pitch excitation moment, with 6.5% reduction in pressure. Circular column shows lowest value for heave excitation force. Further the shapes having biaxial symmetry is showing higher value of pressure, pitch response and moment when compared to other shapes. Both pentagonal and circular can be suggested to be used to control responses.

4. Conclusions

The effect of stepping and tilting is showing a positive influence on the overall response reduction. The effect of change in shape/geometry has suggested us with 4 novel floater models which can be analyzed and compared to further prove its effectiveness using CFD analysis. The five stepped column with four stepped pontoon having a 7.5° outward column tilt can either have pentagonal or circular column shape; and elliptical or square pontoon shape. Four combination with these said above changes are possible. Such a preliminary trial run to reduce the number of model tests for CFD analysis can prove to reduce the computational time and effort. The validity of the following study can be further strengthened through CFD analysis and experimental test done on the most favorable models and specific models having anomalies from the results of FEA analysis.

Acknowledgments

The stipend provided to the first author by the Ministry of Education, Government of India for pursuing full-time M.Tech is gratefully acknowledged.

References

Domala, V., Ranjeet, M. and Sharma, R. (2014), "A note on effect of geometric dimensions, shape and arrangement of columns and pontoons on heave and pitch response of semi-submersible", In 2014 Oceans-St. John's, 1-10. IEEE. https://doi.org/10.1109/OCEANS.2014.7003061.

Global Offshore Wind Report 2023. https://gwec.net/wp-content/uploads/2023/08/GWEC-Global-Offshore-Wind-Report-2023.pdf.

Jonkman, J.M. (2009), "Dynamics of offshore floating wind turbines—model development and verification", Wind Energy: An International Journal for Progress and Applications in Wind Power Conversion Technology, 12(5), 459-492. https://doi.org/10.1002/we.347.

Liu, Z., Zhou, Q., Tu, Y., Wang, W. and Hua, X. (2019), "Proposal of a novel semi-submersible floating wind turbine platform composed of inclined columns and multi-segmented mooring lines", *Energies*, **12**(9), 1809. https://doi.org/10.3390/en12091809.

Ma, Y., Hu, C., Zhou, B., Li, L. and Kang, Y. (2019), "Hydrodynamic analysis of a semi-submersible wind-tidal combined power generation device", *J. Mar. Sci. Appl*., **18**, 72-81.https://doi.org/10.1007/s11804-019-00073-x.

Otter, A., Murphy, J., Pakrashi, V., Robertson, A. and Desmond, C. (2022), "A review of modelling techniques for floating offshore wind turbines", *Wind Energy*, **25**(5), 831-857. https://doi.org/10.1002/we.2701.

Rajeswari, K. and Nallayarasu, S. (2021), "Hydrodynamic response of three-and four-column semi-submersibles supporting a wind turbine in regular and random waves", *Ships Offshore Struct.*, **16**(10), 1050-1060. https://doi.org/10.1080/17445302.2020.1806681.

Rajeswari, K. and Nallayarasu, S. (2022), "Experimental and numerical investigation on the suitability of semi-submersible floaters to support vertical axis wind turbine", *Ships Offshore Struct.*, **17**(8), 1743-1754. https://doi.org/10.1080/17445302.2021.1938800.

Sethuraman, L. and Venugopal, V. (2013), "Hydrodynamic response of a stepped-spar floating wind turbine: Numerical modelling and tank testing", *Renew. Energ.*, **52**, 160-174. https://doi.org/10.1016/j.renene.2012.09.063.

Shokouhian, M., Head, M., Seo, J., Schaffer, W. and Adams, G. (2021), "Hydrodynamic response of a semi-submersible platform to support a wind turbine", *J. Mar. Eng. Technol.*, **20**(3), 170-185. https://doi.org/10.1080/20464177.2019.1571662.

Subbulakshmi, A., Verma, M., Keerthana, M., Sasmal, S., Harikrishna, P. and Kapuria, S. (2022), "Recent advances in experimental and numerical methods for dynamic analysis of floating offshore wind turbines—An integrated review", *Renew. Sustain. Energ. Rev.*, **164**, 112525. https://doi.org/10.1016/j.rser.2022.112525.

Zhang, H., Wang, H., Cai, X., Xie, J., Wang, Y. and Zhang, N. (2022), "Research on the dynamic performance of a novel floating offshore wind turbine considering the fully-coupled-effect of the system", *J. Mar. Sci. Eng.*, **10**(3), 341. https://doi.org/10.3390/jmse10030341.

MK